Available online www.jsaer.com

Journal of Scientific and Engineering Research, 2015, 2(2):23-39

Research Article

ISSN: 2394-2630
CODEN(USA): JSERBR

Kinetic, Isotherm and Thermodynamic Modelling on the Adsorptive Removal of Malachite Green on *Dacryodes edulis* Seeds

Igwegbe CA*[1], Onyechi PC[2], Onukwuli OD[1]

[1]Department of Chemical Engineering, Nnamdi Azikiwe University, Awka, Nigeria.
[2]Department of Industrial and Production Engineering, Nnamdi Azikiwe University, Awka, Nigeria.

Abstract The kinetics, isotherms and thermodynamics of the removal of malachite green on *Dacryodes edulis* seeds have been studied. The adsorbent was prepared by chemical activation methods using phosphoric acid and sodium chloride. Their properties were determined and their removal efficiencies on malachite green were compared. The effect of particle size, adsorbent dose, and initial pH of solution, adsorbate concentration and contact time on the process of adsorption was investigated. The experimental data were modeled using linear regression method of analysis. The coefficient of determination was used for model adequacy. Standard error of estimate was used to validate the pseudo kinetic models. The pseudo second-order kinetic model was found to best correlate the experimental data. The intra-particle diffusion is not the only rate controlling step in the process. The experimental data were found to follow the Langmuir, Freundlich and Tempkin isotherm models. The negative free energy indicated that the adsorption processes were spontaneously feasible. The process of adsorption has been found to be endothermic in nature**.** From the study it was deduced that the *Dacryodes edulis* activated with phosphoric acid was a better adsorbent than the sodium chloride activated sample and the phosphoric acid is a better activating and porosity increasing agent.

Keywords Activation, Adsorption, *Dacryodes edulis* seeds, Kinetics, Isotherm, Malachite green, Activated Carbon.

1. Introduction

One of the greatest problems of the contemporaneous society is the contamination of water caused by dye molecules [1]. Color is the first pollutant to be known in wastewater [2]. Malachite green (MG) is a cationic dye and is widely used for the dyeing of leather, wool and silk, distilleries, jute, paper, as a food-coloring agent, food additive, in medical disinfectant and fish industries [3]. MG dye is known to cause carcinogenesis, mutagenesis, teratogenesis and respiratory toxicity [4]. Various techniques have been employed for the removal of dyes from wastewaters which include adsorption, nano-filtrtion, electro kinetic coagulation, coagulation and precipitation, advanced chemical oxidation, electrochemical oxidation, ozonation, supported liquid membrane, liquid-liquid extraction and biological process [5]. Adsorption has been shown to be one of the most promising and extensively used methods for the removal of both inorganic and organic pollutants from contaminated water [6]. The use of activated carbon has been highlighted as an effective technique for dye removal due to its unique molecular structure, high porosity and an extensive surface area which make them effective adsorbents for several toxic materials in wastewater treatment [7].

Dacryodes edulis (Figure 1), a flowering plant is a fruit tree native to Africa, sometimes called African pear, nsafu, bush butter tree, or native pear. It is called ube igbo by the igbos in the southeast of Nigeria. *Dacryodes edulis* is an evergreen tree attaining a height of 18–40 m in the forest but not exceeding 12 m in plantations. It has a relatively short trunk and a deep, dense crown. Native pear, *Dacryodes edulis* is widely found in many sub-Saharan countries including Nigeria, Liberia, Cameroon and Zaire [8].

Figure 1: *Dacryodes edulis fruits and seeds*

Adsorption studies have been made using different adsorbents on the removal of malachite green dye such as rubber seed coats [9, 10], rambutan peels [4], ginger waste [3], degreased coffee bean [11], rattan sawdust [12] and rice husks [13].

The objective of this study is to investigate the kinetics, isotherm and thermodynamics on the malachite green from aqueous solution using activated carbon produced from *Dacryodes edulis* seed shells which is an abundant waste in Southeast, Nigeria using different chemical activation methods. The removal efficiencies of the adsorbents (PAAC and PSAC) on MG removal at the same conditions will be compared.

2. Materials and Methods

2.1. Preparation of the adsorbents

Dacryodes edulis seeds (APS) were collected from Awka, Anambra state, Nigeria environs and washed thoroughly with de-ionized water to remove dirt, dried in the oven at 105 ºC. The APS were ground, sieved to the desired particle size of 1-2mm. A portion of the sample was soaked in 60% orthophosphoric acid (H_3PO_4) acid and another in sodium chloride (NaCl) for 24 hours at room temperature and carbonized at 500 ºC for 3 hours using muffle furnace (Model SX-2.5-10). The carbonized samples were washed with de-ionized water until pH 7, filtered and dried in the oven at 105 ºC for 8 hours. The dried sample was allowed to cool to room temperature, sieved to different particle sizes and stored in air tight container for adsorption studies. The produced carbon is shown in figure 2.

Figure 2 *Carbonized Dacryodes edulis seeds*

2.2. Characteristics of the adsorbents

The physicochemical properties of the adsorbents (PAAC and PSAC) were determined using methods described by [14]. X-ray Fluorescence (XRF) was used to determine the oxides present in the untreated carbon (UPS) using Munipal 4 model XRF spectrometer. The Fourier transforms infrared (FTIR) was used to determine the functional groups present in UPS, PAAC and PSAC using Shimadzu S8400 spectrophotometer, with samples prepared by the conventional KBr disc method. X-ray diffraction (XRD) was used to determine the diffraction pattern and inter planar spacing of PAAC and PSAC. XRD patterns of carbons were obtained on a powder X-ray diffractometer (Stchmabzu model 6000) with CuKα radiation having a scanning speed of 8.000 deg/min and tested at 40.0 kV and 30 mA. The patterns were recorded over a 2-theta (2θ) range of 2.0000 – 60.0000 deg. Scanning Electron Microscopy (SEM) was used to determine the surface morphology of PAAC and PSAC.

2.3. Adsorption studies

Malachite green (MG) of analytical grade was used without further purification. 0.1g of the dye was dissolved in 1000ml of de-ionized water to get a dye solution of 100mg/l. Dye adsorption experiments were performed by taking 100 ml stock solution of dye and treated with a known dose of adsorbent at 120 rev/min. After a desired time of treatment, the dye solution was centrifuged and the concentration of the residue was determined using UV-vis spectrophotometer (Model UV 754) at λ_{max} = 617nm. The effects of particle size, pH, adsorbent dose, concentration and contact time on the process of adsorption were investigated. The amount of dye adsorbed per unit mass of activated carbon (mg/g) and percentage adsorbed (%) were obtained as follows:

$$q_e = \frac{(C_o - C_e)V}{W} \quad (1)$$

$$\text{Percentage adsorded} = \frac{Co - Ce}{Co} \times 100 \quad (2)$$

where C_0 is the initial concentration of MG in the solution (mg/l); C_e is the final concentration of MG in the solution (mg/l); V is the volume of the solution (l); and W is the weight of carbon (g).

The coefficient of determination (R^2) was used to determine the applicability and acceptance of the isotherm and kinetic models. The sum of the squares error (SSE %) was also used to determine the adequacy of fit of the pseudo first order and pseudo second order kinetic models. The higher the R^2 value and the lower the value of SSE (%), the better the adequacy of fit of the model. The SSE was estimated as follows [9]:

$$\text{SSE (\%)} = \frac{\sqrt{\Sigma(q_{e(exp)} - q_{e(cal)})^2}}{N} \quad (3)$$

3. Results and discussion

3.1. Physicochemical properties of the adsorbents

The physicochemical properties of the adsorbent are presented in table 1. The PAAC was found to have a higher surface area indicating a higher adsorptive performance than PSAC. X-ray Fluorescence (XRF) was used to determine the oxides present in the APS. The oxides present in the adsorbent which may be attributed to adsorption study are shown in table 2. The oxides of calcium and phosphorus are the major constituents of the adsorbents indicating that the *Dacryodes edulis* seeds can be a source of obtaining useful elements. The FTIR analysis was used to examine the surface functional groups of the adsorbents and to identify those groups responsible for dye adsorption. The FTIR spectra of UPS, PAAC and PSAC are shown in figures 3-5 (plot of IR transmittance against wave number**)**. Their frequencies of the bands and the corresponding functional groups are presented in tables 3-5. The O-H stretch in alcohols which is a very strong and broad bond can be detected in the carbons which are important adsorption sites. The modifications in the frequencies of the bands present in UPS may be as a result of chemical activation and reactions with O-H groups. Some of the bands and intensities were shifted or removed and new peaks were also detected after reaction with the activating agents indicating a change in the crystalline structure of the carbon (UPS). Xray diffraction (XRD) has been used to determine the diffractive pattern present on PAAC and PSAC. The XRD spectrum of the carbons showed broad peaks (Figure 6-7), which indicates the presence of high content of amorphous form of carbon and little amounts of crystalline materials in the adsorbents. The three strongest peaks present in PAAC and PSAC, with their interplanar spacings (d) and 2-Theta value (2Ɵ) are presented in tables 6 and 7 respectively. The SEM micrographs of PAAC and PSAC are presented as figures 8 and 9 respectively. Both figures seem to be rough with spongelike protrusions. High level of porosity was observed on PAAC and PSAC. The PAAC was found to be more porous

than the PSAC which will show the MG will be more adsorbed by PAAC and H_3PO_4 increased the porosity than NaCl. The higher surface area for PAAC also supported its porosity than PSAC.

Table 1: Physicochemical properties of PAAC and PSAC

Property	PAAC	PSAC
Moisture content (%)	9.3	7.8
Ash content (%)	5.47	6.22
Volatile matter (%)	17.40	17.53
Fixed carbon (%)	77.13	76.25
Bulk density (g/cm^2)	0.46	0.45
pH	6.7	7.4
Iodine number (mg/g)	717	699
Surface area (m^2/g)	841	739
Yield	25.7	26.1

Table 2: XRF results of APS

Chemical constituent	Composition (%)
K_2O	74.86
CaO	16.8
SO_3	8.52
Ag_2O	7.86
P_2O_5	7.79
SeO_2	4.78
Fe_2O_3	1.90
Re_2O_7	1.90
ZnO	1.22
Yb_2O_3	0.20
BaO	0.39
MnO	0.29
TiO_2	0.30
CuO	0.25
NiO	0.09

Table 3: Fourier transform infrared spectrum for UPS

Wave number (cm^{-1})	Bond source	Functional group
606.63	C–Cl stretch	Alkyl halides
1547.93	N–O asymmetric stretch	Nitro compounds
2264.51	–C≡C– stretch	Alkynes
2433.28	–C≡C– stretch	Alkynes
3463.30	O–H stretch	Alcohols and phenols
3620.51	O–H stretch	Alcohols and phenols
3760.35	O–H stretch	Alcohols and phenols
3873.19	O–H stretch	Alcohols and phenols

Table 4: Fourier transform infrared spectrum for PAAC

Wave number (cm^{-1})	Bond source	Functional group
631.71	C–Cl stretch	Alkyl halides
1037.74	C–N stretch	Aliphatic amines
1422.55	C–C stretch	Aromatics
1537.32	N– O asymmetric stretch	Nitro compounds
2258.72	–C≡C– stretch	Alkynes
2965.65	C–H stretch	Alkanes
3425.69	O–H stretch	Alcohols and phenols
3904.05	O–H stretch	Alcohols and phenols

Table 5: Fourier transform infrared spectrum for PSAC

Wave number (cm^{-1})	Bond source	Functional group
639.42	C–Cl stretch	Alkyl halides
865.10	=C–H bend	Alkenes
1009.77	C–O stretch	Alcohols, carboxylic acids, esters, ethers
1415.80	C–C stretch	Aromatics
1531.53	N–O asymmetric stretch	Nitro compounds
1833.40	C=O stretch	Amides, ketones, aldehydes, carboxylic acid, esters
2265.47	–C≡C– stretch	Alkynes
3429.55	O–H stretch	Alcohols and phenols
3874.16	O–H stretch	Alcohols and phenols

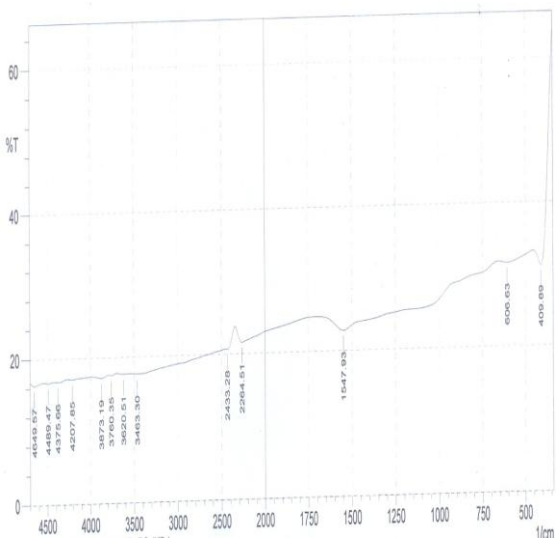

Figure 3: *FTIR spectrum of UPS*

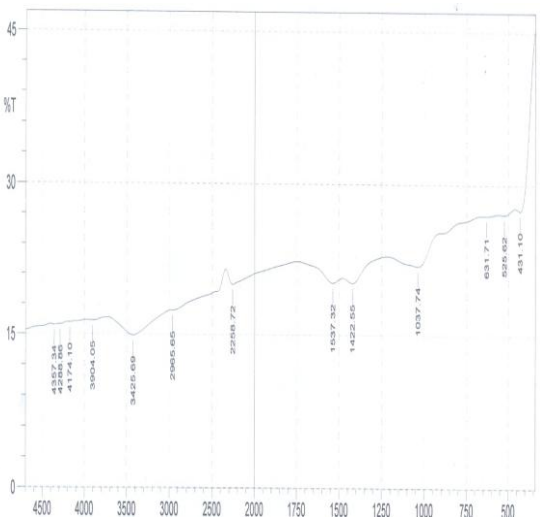

Figure 4: *FTIR spectrum of PAAC*

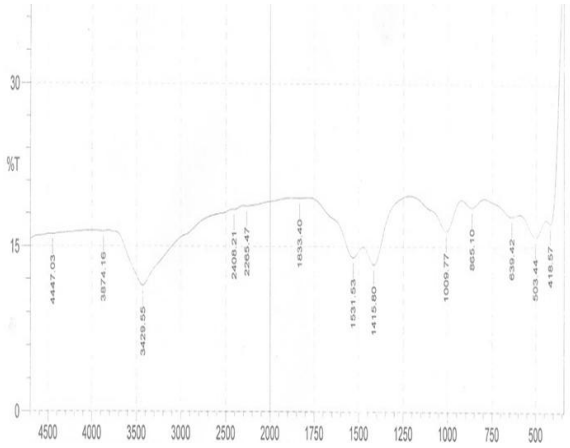

Figure 5: *FTIR spectrum of PSAC*

Table 6: Interplanar spacing, d of X-rays reflections for PAAC

d (Å)	2-Theta Value
4.59880	19.2850
4.19055	21.1845
3.91990	22.6659

Table 7: Interplanar spacing, d of X-rays reflections for PSAC

d (Å)	2-Theta Value
5.31047	16.6807
5.07542	17.4591
4.30788	20.6011

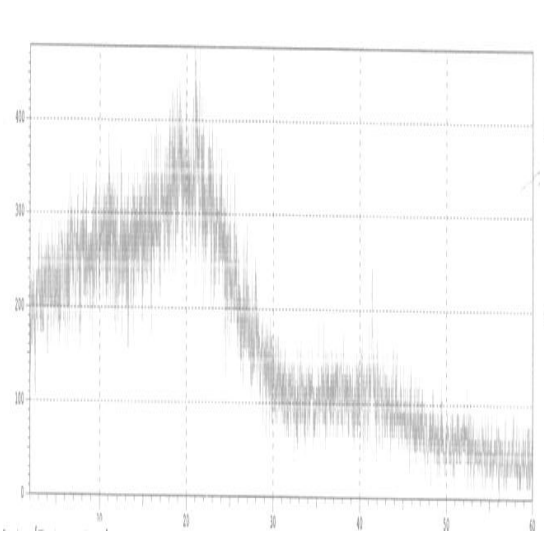

Figure 6: *XRD profile of PAAC*

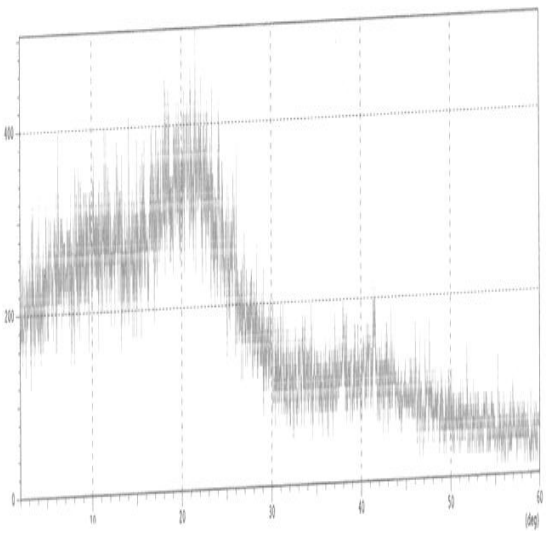

Figure 7: *XRD profile of PSAC*

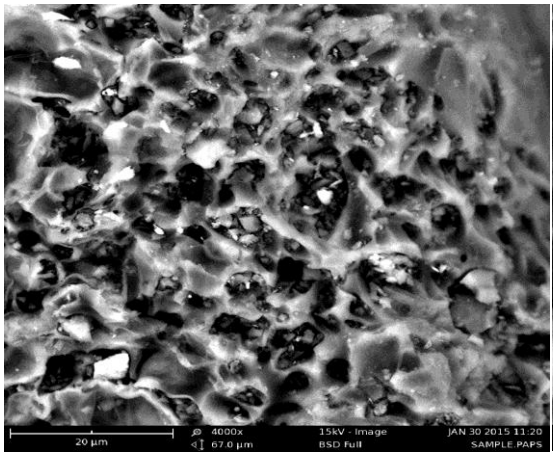

Figure 8: *SEM image on PAAC.*

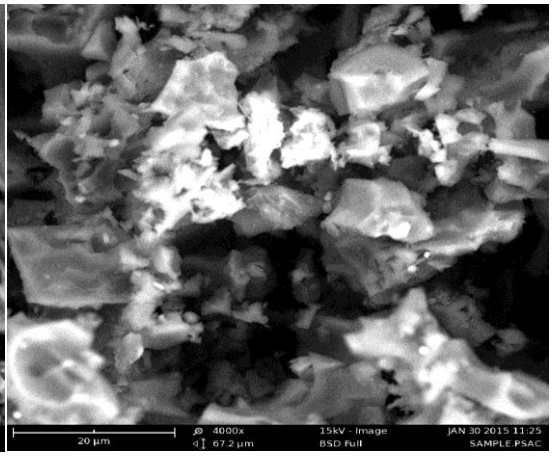

Figure 9: *SEM image on PSAC.*

3.2. Batch adsorption studies

3.2.1. Effect of particle size

Figure 10 shows that the percentage of MG adsorbed decreased with increase in particle size of the adsorbents. This may be as a result of decreasing the particle size improves the pores available for adsorption.

3.2.2. Effect of initial pH of solution

Figure 11 shows that higher uptakes of MG by PAAC and PSAC was obtained at pH of 10. The increase in the percentage adsorbed as the pH was decreased may be caused by the electrostatic interaction between negatively charge adsorbent and cationic MG [3].

3.2.3. Effect of adsorbent dose

The percentage adsorbed increased as the adsorbent dose was increased until saturation point was reached (Figure 12). This may be as a result of increase in the number of active sites available for the process of adsorption which nearly becomes constant as the dosage was increased further This may be due to sites remaining unsaturated during the adsorption process [15].

3.2.4. Effect of adsorbate concentration

Figure 13 shows that the percentage removal of the adsorbates decreased as the adsorbate concentration was increased. This may be at higher concentration, the number of dye ions competing for the available sites on the surface of adsorbent was high resulting in high percentage adsorbed [9].

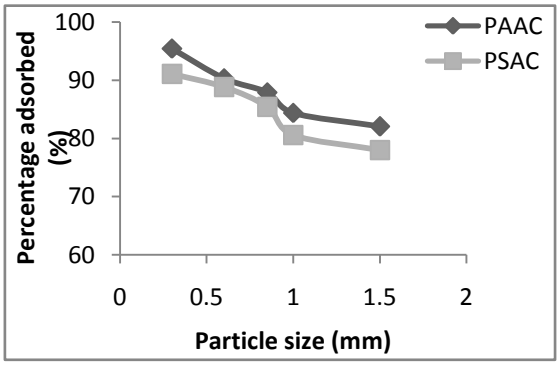

Figure 10: *Effect of particle size on percentage adsorbed*

3.2.5. Effect of contact time

The percentage adsorbed increased with increasing the contact time (Figure 14). The rate of removal of the adsorbate was rapid in the beginning due to the number of active sites available for the adsorption of dye ions and after a certain time, only a very low increment was observed.

Dosage = 1g, Concentration = 100mg/l, Time = 60min, Temperature = 303K

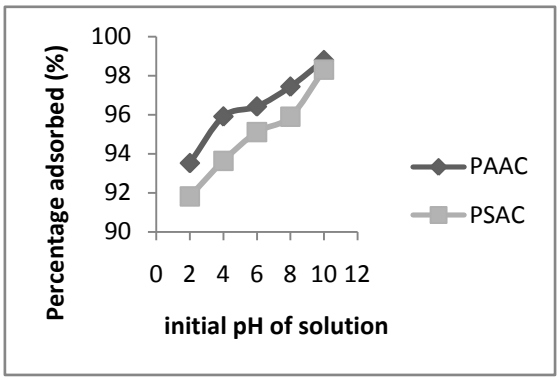

Figure 11: *Effect of initial pH of solution on percentage adsorbed.*
Particle size = 0.30mm, Dosage = 1g, Concentration = 100mg/l, Time = 60min, Temperature = 303K

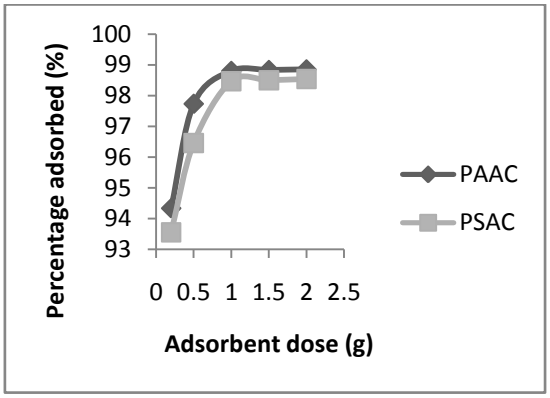

Figure 12: *Effect of adsorbent dose on percentage adsorbed.*
Particle size = 0.30mm, pH = 10, Concentration = 100mg/l, Time = 60min, Temperature = 303K

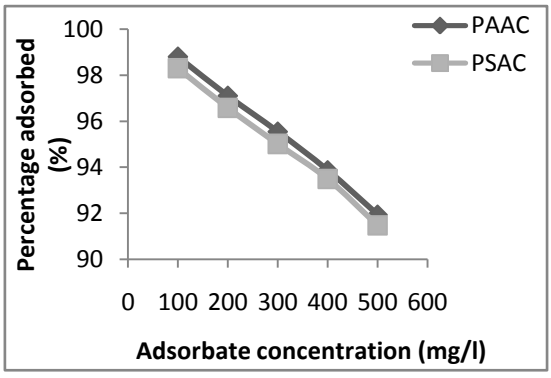

Figure 13: *Effect of adsorbate concentration*
Particle size = 0.30mm, pH = 10, Dosage = 1g, Time = 60min, Temperature = 303K

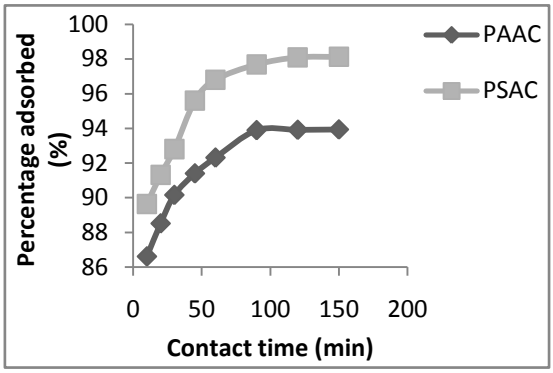

Figure 14: *Effect of contact time on percentage adsorbed.*
Particle size = 0.30mm, pH = 10, Dosage = 1g, Concentration = 100mg/l, Temperature = 303K

3.3. Adsorption Kinetics

The kinetics was studied in order to know the mechanism of the adsorption process.

3.3.1. Pseudo first-order kinetic model

The pseudo-first-order Lagergren equation is given by [16]:

$$\frac{dq_t}{dt} = k_1 (q_e - q_t) \qquad (4)$$

Integration under the boundary conditions of t = 0 to t = t and $q_t = 0$ to $q_t = q_t$, gives a linear expression:

$$\log(q_e - q_t) = \log q_e - \frac{K_1}{2.303} t \qquad (5)$$

where q_t and q_e are the amounts of MG adsorbed at time t and equilibrium respectively and k_1 (min^{-1}) is the pseudo-first-order rate constant for the process of adsorption. K_1 and q_e were determined from the slope and intercept of the plot of log ($q_e - q_t$) versus t (Figure 15).

The pseudo first order rate constants, K_1 is given in table 8. The values of the correlation coefficients (R^2) of 0.974 and 0.950 for PAAC and PSAC respectively indicate that the removals of MG on PAAC and PSAC follow the pseudo first – order kinetic model. The low SSE values of 2.743 and 2.656 for PAAC and PSAC respectively indicates goodness of fit and adequacy of the model.

3.3.2. Pseudo second-order kinetic model

The pseudo second – order adsorption kinetic equation is expressed as [17]:

$$\frac{t}{q_t} = \frac{1}{k_2} + \frac{1}{q_e} t \qquad (6)$$

k_2 is the rate constant of pseudo second order adsorption (g/mg/min).The values of k_2 and q_e (table 8) were calculated from the plots of t/q_t versus t as shown in figure 16. The R^2 values which are close to unity (0.999) shows that the adsorption of MG on PAAC and PSAC is best described by the pseudo second-order mechanism suggesting that the rate-limiting step is a chemical adsorption [18]. The low SSE values of 0.280 and 0.316 for PAAC and PSAC respectively indicates goodness of fit and adequacy of the model.

3.3.3. Elovich model

The Elovich kinetic model is expressed as [19]:

$$\frac{t}{q_t} = \alpha \exp(-b\, q_e) \qquad (7)$$

Integration of this equation for the boundary conditions, gives:

$$qt = (1/\beta) \ln (\alpha b) + (1/\beta) \ln t \qquad (8)$$

where α is the initial adsorption rate (mg/g min) and β is related to the extent of surface coverage and the activation energy for chemisorptions (g/mg). A plot of q_t versus In t yielded a linear relationship (Figure 17)

where the Elovich constants, β and α were obtained and presented in table 8. The adsorption conformed to the Elovich kinetic model since the values of the linear regression coefficients (R^2) are close to unity (table 8).

3.3.4. Intraparticle diffusion kinetic model

The intraparticle diffusion model equation is given by [20]:

$$q_t = k_{pi}\, t^{0.5} + C_i \qquad (9)$$

where k_{pi} is the rate parameter of stage i and C_i is the thickness of the boundary layer. The plot of q_t versus $t^{0.5}$ (Figure 18) gives a straight line. The intraparticle diffusion is not the only rate controlling step involved in the adsorption of MG by the adsorbents since its linear plots did not pass through the origin [21].

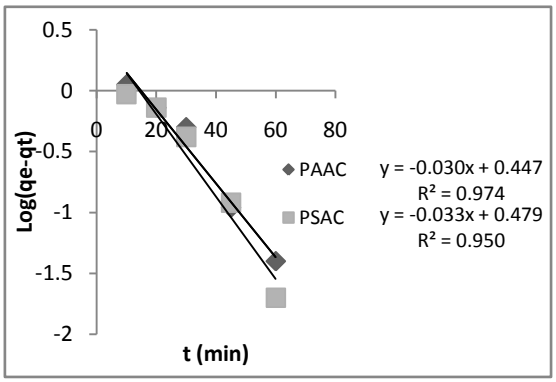

Figure 15: *Pseudo-first order kinetic model on MG adsorption on PAAC and PSAC*

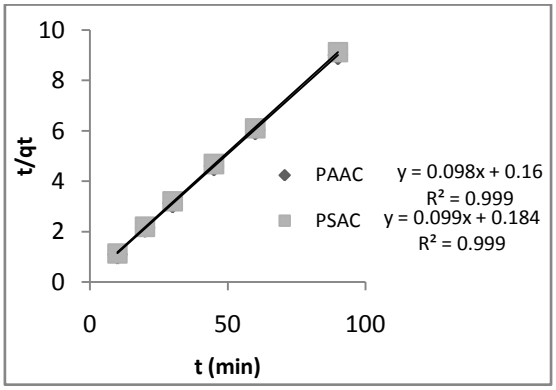

Figure 16: *Pseudo-second order kinetic model on MG adsorption on PAAC and PSAC*

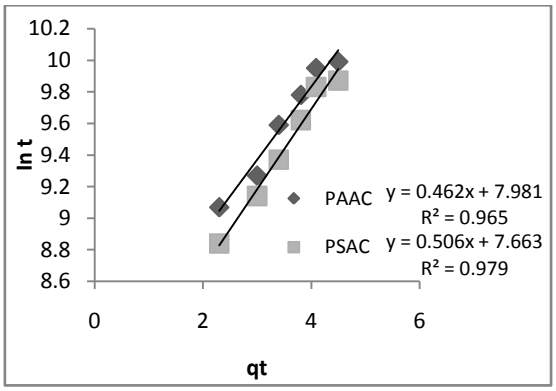

Figure 17: *Elovich kinetic model on MG adsorption on PAAC and PSAC*

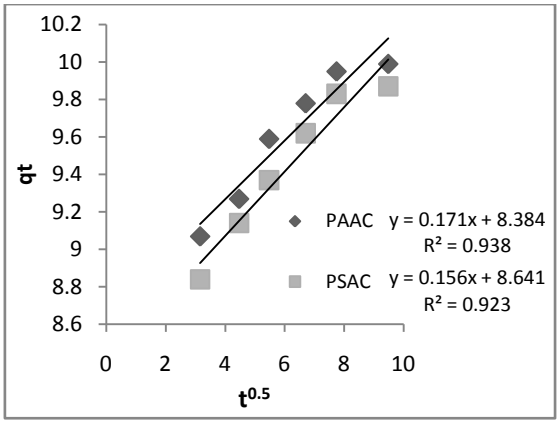

Figure 18: *Intraparticle diffusion model on MG adsorption on PAAC and PSAC*

Table 8: Kinetic parameters obtained for the adsorption of MG on PAAC and PSAC at 303K.

Kinetic model	**PAAC**	**PSAC**
Pseudo first-order		
K_1 (min^{-1})	0.0691	0.0760
qe (mg/g)	2.7990	3.0130
R^2	0.974	0.950
SSE (%)	2.743	2.656
Pseudo Second-order		
k_2(g/mg/min)	0.0598	0.0483
qe (mg/g)	10.1010	10.2041
R^2	0.999	0.999
SSE (%)	0.280	0.316
Elovich		
α (mg/g min)	$1.55x10^7$	$1.07x10^6$
β (g/mg)	2.1978	1.9084
R^2	0.980	0.985
Intra particle and film diffusion		
k_{pi} (mg g^{-1} $min^{-0.5}$)	0.154	0.178
C_i	8.536	8.351
R^2	0.944	0.950

3.4. Adsorption Isotherm

3.4.1. Langmuir isotherm

The lineralized Langmuir model is expressed as [19]:

$$\frac{C_e}{q_e} = \frac{C_e}{Q_m} + \frac{1}{Q_m K_L} \qquad (10)$$

where C_e is the equilibrium concentration of dye (mg/l) and q_e is the amount of the dye adsorbed (mg) per unit of activated carbon (g). Q_m and K_L are the Langmuir constants related to the adsorption capacity (mg/g) and the equilibrium constant (l/mg) respectively. The separation factor (R_L) is used to predict whether an adsorption process is favourable or unfavourable which can be determined as follows [2]:

$$R_L = \frac{1}{1 + K_L C_0} \qquad (11)$$

where K_L is a Langmuir constant. R_L value implies the adsorption to be unfavourable ($R_L > 1$), linear ($R_L = 1$), favourable ($0 < R_L < 1$), or irreversible ($R_L = 0$). The plot of C_e/q_e against C_e is shown in figure 19. The correlation coefficients (R^2) of 0.974 and 0.968 for PAAC and PSAC respectively showed that the adsorption conformed to the Langmuir model. The separation factors, R_L of 0.0849 and 0.1076 for PAAC and PSAC respectively were found to be less than one indicating favourable adsorption (table 9).

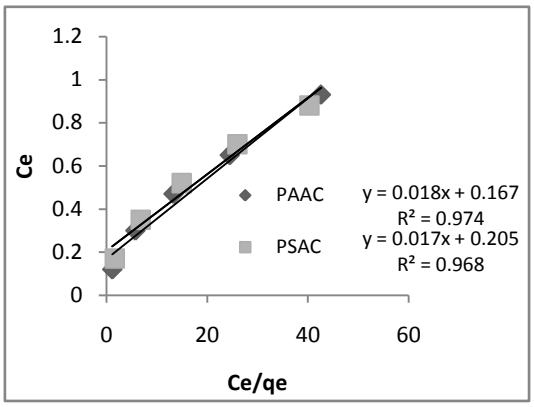

Figure 19: *Langmuir isotherm model on MG adsorption on PAAC and PSAC*

3.4.2. Freundlich isotherm

Freundlich isotherm can be expressed as [22]:

$$q_e = K_F C_e^{\frac{1}{n}} \quad (12)$$

This equation can be linearized as:

$$\log q_e = \frac{1}{n}\log C_e + \log K_F \quad (13)$$

The respective Freundlich constants, n and k_f (table 9) were calculated from the slopes and intercepts of the linear plots (Figure 20) of log q_e versus log C_e. The values of k_f (measure of adsorption) increased with increasing temperature. The R^2 values of 0.999 and 0.996 for PAAC and PSAC respectively obtained shows that the adsorption of MG conformed to the Frendlich isotherm generally.

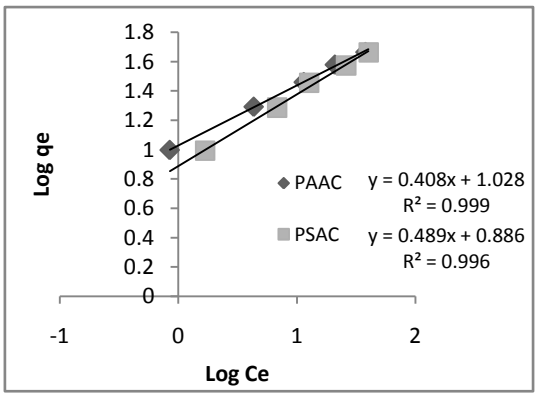

Figure 20: *Freundlich isotherm model on MG adsorption on PAAC and PSAC*

3.4.3. Temkin isotherm

The Temkin isotherm is expressed as [23]:

$$q_e = \frac{RT}{b} \ln (K_T C_e) \quad (14)$$

The linear form of this isotherm can be given by

$$q_{e} = \frac{RT}{b} \ln K_T + \frac{RT}{b} \ln C_e \quad (15)$$

q_e is the amount adsorbed at equilibrium in mg/g; k_1 is the Temkin isotherm energy constant. The constants b_T which is related to the heat of adsorption and K_T which is the equilibrium binding constant corresponding to the maximum binding energy were determined from the plot of q_e versus in C_e (Figure 21). The constants are presented in table 9. The high values of b_T of 253.36 and 225.93 J/mg for PAAC and PSAC respectively indicate that the interaction between the adsorbate and the adsorbent was strong. The correlation coefficients, R^2 value of 0.956 and 0.951 for PAAC and PSAC respectively indicate that the isotherm model fitted well to the equilibrium adsorption experimental data.

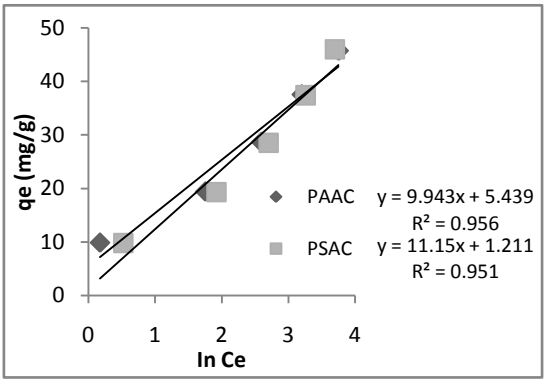

Figure 21: *Temkin isotherm model on MG adsorption on PAAC and PSAC*

3.4.4. Dubinin–Radushkevich isotherm

The Dubinin-Radushkevich isotherm is given as [24]:

$$\ln q_e = \ln q_D - B\varepsilon^2 \quad (16)$$

$$\varepsilon = RT \ln (1+1/C_e) \quad (17)$$

$$E = 1/(2B)^{1/2} \quad (18)$$

where q_D is the theoretical saturation capacity (mg/g), B is a constant related to mean free energy of adsorption per mole of the adsorbate (mol^2/J^2), ε is the polanyi potential, R is the universal gas constant (8.314 J/mol/K) and T is the temperature in Kelvin and E is the mean sorption energy. The D-R isotherm constants B, qe and E were obtained (table 9) from the linear plots of In qe against ε^2 (figure 22). The correlation coefficients, R^2 of 0.769 and 0.779 for PAAC and PSAC respectively obtained showed that the experimental data obtained did not fit well to the D–R isotherm (table 9). The removal of MG on the adsorbents is not a physical process since the values of mean free energy (E) obtained were found to be < 8KJ/mol [25].

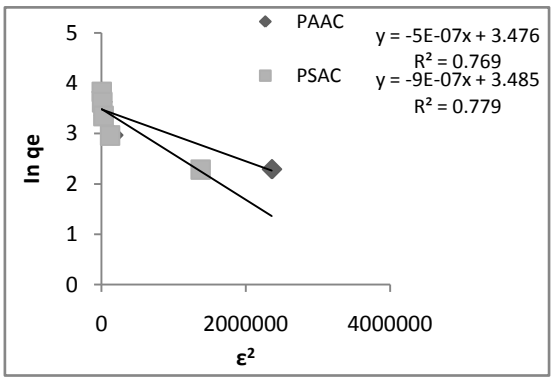

Figure 22: *Dubinin Ruduskevich isotherm model on MG adsorption on PAAC and PSAC*

Table 9: Calculated isotherm parameters for MG adsorption on PAAC and PSAC at 303K

Isotherm model	PAAC	PSAC
Langmuir		
Q_m (mg/g)	55.56	58.82
b (L/mg)	0.1078	0.0829
R_L	0.0849	0.1076
R^2	0.974	0.968
Freundlich		
N	2.3041	2.0534
K_f (L/g)	9.1622	7.6033
R^2	0.999	0.996
Tempkin		
b_T (J/mg)	253.36	225.93
A	1.7281	1.1147
R^2	0.956	0.951
Dubinin-Radushkevich		
q_D (mg/g)	32.330	32.622
B (mol^2/KJ^2)	5×10^{-7}	9×10^{-7}
E (kJ/mol)	0.0001	0.0001
R^2	0.769	0.779

3.5. Adsorption Thermodynamics

The activation energy was evaluated from the pseudo second-order kinetic rate constants obtained from adsorptive removals performed at 303, 313 and 323K. The Arrhenius equation is given as [26]:

$$\ln k_2 = \ln A - \frac{Ea}{RT} \qquad (19)$$

where k_2 is the rate constant obtained from the pseudo second-order kinetic model (g/mg h), Ea is the Arrhenius activation energy of adsorption (kJ/mol) and A is the Arrhenius factor. In k_2 was plotted against 1/T and Ea was obtained from the slope. The activation energies of adsorption of MG on PAAC and PSAC are 86.3964 and 64.0486 K/Jmol respectively which are greater than 40K/Jmol which implies that the rate-limiting step might be a chemically controlled process [25].

Adsorption thermodynamics is the study of the effect of temperature on the process of adsorption. ΔG^0 and ΔH^0 were used to evaluate the spontaneity and nature of the adsorption process respectively [23]. The thermodynamic parameters free energy (ΔG^0), enthalpy (ΔH^0) and entropy (ΔS^0) were determined as follows [27]:

$$\ln K_C = \frac{\Delta S^0}{R} - \frac{\Delta H^0}{RT} \qquad (20)$$

$$\Delta G^0 = -RT \ln K_C \qquad (21)$$

where R (8.314 J/mol K) is the universal gas constant, T (K) is the solution temperature and K_L (L/mg) is the Langmuir isotherm constant. The values of ΔH° and ΔS° were calculated, respectively from the slope and intercept of the Vant Hoff plot of ln K_C versus 1/T (Figure 23) are presented in table 10.

The values of ΔG^0 were found to be negative which decreased with increased temperature showing that the adsorption was more favourable and spontaneous at higher temperature (table 10). The positive value of ΔH^0 indicates the endothermic nature of the process. The positive value of ΔS^0 indicates an increase in the randomness at the solid/solution interface due to the redistribution of energy between MG and the adsorbents [28]. The removal of MG with PAAC was found to be more spontaneous than with PSAC.

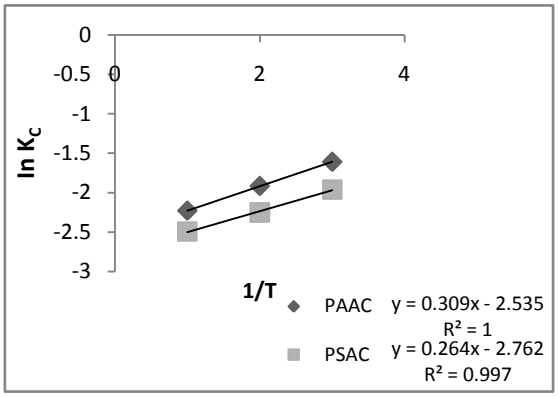

Figure 23: *Vant Hoff plot on MG adsorption on PAAC and PSAC*

Table 10: Thermodynamic parameters for the adsorption of MG dye on PAAC and PSAC

Adsorbent	Ea (KJ/mol)	ΔH^0 (KJ /mol)	ΔS^0 (J /K /mol)	R^2	ΔG^0 (KJ /mol)		
					303K	313K	323K
PAAC	86.3964	25.615	65.947	1.000	-19.956	-20.616	-21.275
PSAC	64.0486	21.816	51.173	0.997	-15.484	-15.995	-16.508

Particle size = 0.3mm, Contact time = 60 min, Initial concentration=100 mg/L, Initial pH =10, and adsorbent dose=1g.

4. Conclusions

In this study activated carbon prepared from *Dacryodes edulis* seeds using chemical activations was used for the removal of MG from aqueous solution. The removal efficiencies of using H_3PO_4 activated carbon (PAAC) and NaCl activated carbon (PSAC) were compared. The batch adsorption studies indicated that the percentage adsorbed depends on particle size, adsorbent dose, pH, contact time and adsorbate concentration. The pseudo second order kinetic was found to best correlate the experimental data obtained. The intraparticle diffusion is involved in the adsorption of MG by the adsorbents but it is not the only rate controlling step. The adsorption of PAAC and PSAC on MG was found to follow the Langmuir, Freundlich and Tempkin isotherms. The negative free energy change (ΔG^0) and positive value of entropy ($\Delta S\circ$) indicates the feasible and spontaneous nature of the process. The H_3PO_4 activated carbon (PAAC) was found to be a better adsorbent than the NaCl activated carbon (PSAC) and H_3PO_4 is a better activating agent than NaCl. The thermodynamic and kinetics data can be further used for the design of a plant for treatment of industrial wastewater containing malachite green on large scale.

References

1. Pavan, F. A., Camacho, E. S., Lima, E. C., Dotto, G. L., Branco, V. T., & Dias, S. L. (2014). Formosa papaya seed powder (FPSP): Preparation, characterization and application as an alternative adsorbent for the removal of crystal violet from aqueous phase. *Journal of Environmental Chemical Engineering*, *2*(1), 230-238.
2. Rangabhashiyam, S., Anu, N., & Selvaraju, N. (2013). Sequestration of dye from textile industry wastewater using agricultural waste products as adsorbents. *Journal of Environmental Chemical Engineering*, *1*(4), 629-641.
3. Ahmad, R., & Kumar, R. (2010). Adsorption studies of hazardous malachite green onto treated ginger waste. *Journal of environmental management*, *91*(4), 1032-1038.
4. Ahmad, M. A., & Alrozi, R. (2011). Removal of malachite green dye from aqueous solution using rambutan peel-based activated carbon: Equilibrium, kinetic and thermodynamic studies. *Chemical Engineering Journal*, *171*(2), 510-516.
5. Mahmoud, A. S., Ghaly, A. E., & Brooks, M. S. (2007). Removal of dye from textile wastewater using plant oils under different pH and temperature conditions. *Am. J. Environ. Sci*, *3*(4), 205-218.

6. Prasad, A. L., & Santhi, T. (2012). Adsorption of hazardous cationic dyes from aqueous solution onto Acacia nilotica leaves as an eco friendly adsorbent. *Sustain Environ Res*, *22*(2), 113-22.
7. Isah, U. A., Gatawa, A.I. (2012). A kinetic study of the adsorption of reactive yellow 21 dye on flamboyant shells activated carbon. *Advances in Applied Science Research, 3*(6), 4036- 4040.
8. Arisa, N. U., Lazarus, A. (2008). Production and refining of *Dacryodes edulis* ''native pear'' seeds oil. *African Journal of Biotechnology, 7*(9), 1344 - 1346.
9. Idris, M. N., Ahmada, Z. A., Ahmad M. A., Ahmad N., Sulaiman S. K. (2011). Optimization of process variables for malachite green dye removal using rubber seed coat based activated carbon. *International Journal of Engineering and Technology, 11*(1), 234 - 240.
10. Hameed, B. H., Daud, F. B. M. (2008). Adsorption studies of basic dye on activated carbon derived from agricultural waste: *Hevea brasiliensis* seed coat. *Chemical Engineering Journal, 139*, 48-55.
11. Baek, M. H., Ijagbemi, C. O., Se Jin, O., Kim, D. S. (2010). Removal of malachite green from aqueous solution using degreased coffee bean. *Journal of Hazardous Materials, 176*, 820-828.
12. Hameed, B. H., El-Khaiary, M. I. (2008.) Malachite green adsorption by rattan sawdust: Isotherm, kinetic and mechanism modeling. *Journal of Hazardous Materials 159*, 574–579.
13. Sharma, Y. C., Singh B., Uma. (2009). Fast removal of malachite green by adsorption on rice husk activated carbon. *The Open Environmental Pollution & Toxicology Journal, 1*, 74-78.
14. Nwabanne, J. T., Igbokwe, P. K. (2011). Preparation of activated carbon from nipa palm nut: Influence of preparation conditions. *Research Journal of Chemical Sciences, 1*(6), 53-58.
15. Taha, D. N., Samaka, I. S., Mohammed, L. A. (2013). Adsorptive removal of dye from industrial effluents using natural Iraqi palygorskite clay as low-cost adsorbent. *Journal of Asian Science Research, 3*(9), 945-955.
16. Nwabanne J. T., Igbokwe P. K. (2012) Thermodynamic and Kinetic Behaviors of Lead (II) Adsorption on Activated Carbon Derived from Palmyra Palm Nut. *International Journal of Applied Science and Technology, 2*(9), 245-254.
17. Ahmad, M. A., Herawan, S. G., Yusof, A. A. (2014). Equilibrium, Kinetics, and Thermodynamics of Remazol Brilliant Blue R Dye Adsorption onto Activated Carbon Prepared from Pinang Frond. Hindawi Publishing Corporation. *Mechanical Engineering* (184265), 1-7.
18. Al-Ghouti, M., Khraisheh, M. A. M., Ahmad, M. N. M., Allen, S. (2005). Thermodynamic behaviour and the effect of temperature on the removal of dyes from aqueous solution using modified diatomite: A kinetic study. *Journal of Colloid Interface Science, 287*,6–13.
19. Okoye, A. I., Ejikeme, P. M., Onukwuli, O. D. (2010). Lead removal from wastewater using fluted pumpkin seed shell activated carbon: Adsorption modeling and kinetics. *International Journal of Environmental Science and Technology, 7*(4), 793-800.
20. Thilagavathi, M., Arivoli, S., Vijayakumaran, V. (2014). Kinetic and Thermodynamic Studies on the Adsorption behavior of Rhodamine B dye using Prosopis Juliflora Bark Carbon. *Scholars Journal of Engineering and Technology, 2*(2B), 258-263.
21. Abramian, L., El-Rassy, H. (2009). Adsorption kinetics and thermodynamics of azo-dye Orange II onto highly porous titania aerogel. *Chemical Engineering Journal, 150*, 403–410.
22. Ugonabo,V. I., Umebamalu, J. C. (2012). Application of agricultural waste in the treatment of industrial waste water. *Journal of Engineering and Applied Sciences, 8*(1), 24-28.
23. Gautam, R. K., Mudhoo, A., Lofrano G., Chattopadhyaya, M. C. (2014). Biomass-derived biosorbents for metal ions sequestration: Adsorbent modification and activation methods and adsorbent regeneration. *Journal of Environmental Chemical Engineering, 2*, 239–259.
24. Ramachandran, P., Vairamuthu, R., Ponnusamy S. (2011). Adsorption Isotherms, Kinetics, Thermodynamics and Desorption Studies of Reactive Orange16 on Activated Carbon Derived From *Ananas Comosus* (L.) Carbon. *Journal of Engineering and Applied Sciences, 6*(11), 15-26.
25. Boparai, H. K., Joseph, M., O'Carroll, D. (2011). Kinetics and thermodynamics of cadmium ion removal by adsorption onto nano zerovalent iron particles. *Journal of Hazardous Materials, 186*, 458-465.

26. Eren, E., Cubuk, O., Ciftci, H., Eren, B., Caglar, B. (2010). Adsorption of basic dye from aqueous solutions by modified sepiolite: Equilibrium, kinetics and thermodynamics study Desalination 252, 88-96.
27. Babakhouya, N., Boughrara, S., Abad F. (2010). Kinetics and Thermodynamics of Cd(II) Ions Sorption on Mixed Sorbents Prepared from Olive Stone and Date Pit from Aqueous Solution. *American Journal of Environmental Sciences, 6*(5), 470-476.
28. Kothiyal, N. C., Sharma, S. **(**2013). Study of Chromium (VI) Adsorption using *Pterospermumacerifolium* Fruit Capsule Activated Carbon (FCAC) and Commercial Activated Charcoal (CAC) as a Selective Adsorbents. *The Holistic Approach to Environment, 32*, 63-82.